

Copy 4
RM SL58H08a

NACA

CLASSIFICATION CHANGED
UNCLASSIFIED

TO: ID 71-242 3-30-71

RESEARCH MEMORANDUM

for the

Bureau of Ordnance, Department of the Navy

EXPERIMENTAL INVESTIGATION OF FLUTTER AND DIVERGENCE

CHARACTERISTICS OF THE ROCKET-MOTOR FIN

OF THE ASROC MISSILE

COORD NO. N-AM-66

By Gilbert M. Levey and Perry W. Hanson

Langley Aeronautical Laboratory
Langley Field, Va.

No. 602(A)	X71-74412	
	(ACCESSION NUMBER)	(THRU)
	13	None
	(PAGES)	(CODE)
	(NASA CR OR TMX OR AD NUMBER)	(CATEGORY)

Restriction/Classification Cancelled

NATIONAL ADVISORY COMMITTEE FOR AERONAUTICS

WASHINGTON

1966-51 1039

NATIONAL ADVISORY COMMITTEE FOR AERONAUTICS

RESEARCH MEMORANDUM

for the

Bureau of Ordnance, Department of the Navy

EXPERIMENTAL INVESTIGATION OF FLUTTER AND DIVERGENCE

CHARACTERISTICS OF THE ROCKET-MOTOR FIN

OF THE ASROC MISSILE*

COORD NO. N-AM-66

By Gilbert M. Levey and Perry W. Hanson

SUMMARY

Some 0.4-scale models of rocket-motor fins of the ASROC missile were investigated for flutter and divergence in the Langley 9- by 18-inch supersonic flutter tunnel in the Mach number range from about 0.6 to 1.3. Results of this investigation indicate that both divergence of the overhung leading edge and flutter occur within the sea-level operating conditions of the missile at Mach numbers above about 1.0. Tests of models with altered root fixity and plan form and of some relatively thicker models indicated that these aeroelastic problems could be overcome either by extending the root clamping plates the entire length of the root chord or by increasing the thickness of the fins by about 25 percent.

INTRODUCTION

At the request of the Bureau of Ordnance, Department of the Navy, an investigation was conducted in the Langley 9- by 18-inch supersonic flutter tunnel on 0.4-scale models of the ASROC rocket-motor fins at Mach numbers from about 0.6 to 1.3. The purpose of this study was to obtain flutter and divergence characteristics. The models were built by the Langley Aeronautical Laboratory and were scaled in such a way that the test dynamic pressures for the models were equal to the full-scale dynamic

pressures. In addition to the 0.4-scale models, other models approximately 25 percent and 45 percent thicker than design thickness and several models having variations in plan form and root fixity were tested.

Test conditions and results of this investigation are presented herein. The Bureau of Ordnance has requested that results of this study be considered proprietary.

SYMBOLS

a	velocity of sound, fps
f_F	flutter frequency, cps
f_n	natural frequency of nth mode ($n = 1, 2, 3, 4$), cps
M	Mach number
q	dynamic pressure, lb/sq ft
t	thickness, in.
T	absolute stagnation temperature, °R
ρ	air density, slugs/cu ft

Subscript:

max maximum

MODEL DESCRIPTION

The basic models used were 0.4-scale replicas made of 2024 aluminum alloy. This scaling was accomplished by multiplying all plan-form dimensions and the thickness of the full-scale model by 0.4, thus making the model thickness a nominal 0.050 inch. In addition to the basic models, some thicker models which had the same plan-form dimensions as the 0.050-inch models but which were 0.063 and 0.072 inch thick (representing a 25-percent and 45-percent increase, respectively, in thickness of the full-scale fin) were tested. Models of the same thickness as the basic models, but with different root fixities and plan form, were also tested. A drawing of the basic model is shown in figure 1(a), and the

variations in root fixities and plan form are shown in figure 1(b). Natural frequencies and thicknesses of the models are presented in table I.

In order to facilitate mounting the model in the wind tunnel, two clamping plates, each equal to the model thickness, were riveted to the model with the same pattern that was used on the full-scale fin. In order to compensate for the possibility that the root restraint on the basic model might not be as good as the root restraint on the full-scale fin, a piece of material was left integral with the model between the two previously mentioned plates. (See fig. 1(a).) At the forward end of the root, a cut was made as shown in figure 1(a) to simulate the fixity of the overhung leading edge. In order to determine the effect of not having this filler piece integral with the main surface, two models (BF-7C and BF-14) were built the same as the full-scale fin would be, with the filler piece butted to the model. (See fig. 1(b).) The models were bolted between two 1/2-inch-steel plates, which in turn were bolted to the wind-tunnel model support.

In most cases, a new model was used for every test because it was found that once the leading edge of a model had diverged, even though it could be straightened and its frequencies did not change, there was an appreciable lowering of the dynamic pressure required for divergence the second time the model was tested. All the data shown in table I pertain to models which had not experienced flutter or divergence prior to the points listed, except for test 33 in which a previously diverged model was used with the overhung leading edge restrained. Test 38 was a rerun of test 37 except for the manner in which the model was clamped. The forward portion of the two clamping plates was cut away as shown in figure 1(b) for test 38.

Typical vibration node lines of the models tested are shown in figure 2, and the natural frequencies for each model are listed in table I. Since the full-scale fin frequencies and nodal patterns are not available, it is not possible to assess the accuracy with which the models simulated the dynamic characteristics of the full-scale fin. Since the basic models used were replicas made of the same material as the full-scale fin, it would be expected that the full-scale frequencies would be 0.4 times the model frequencies.

INSTRUMENTATION

Continuous records of wind-tunnel conditions and model behavior were obtained for each test on an oscillograph. The outputs from pressure cells and from a thermocouple were recorded and used to obtain tunnel static and stagnation pressures and stagnation temperature,

respectively. Strain gages located on the models as shown in figure 1 were used to record the natural frequencies and flutter frequencies of the models as listed in table I. In addition, the forward strain gages were used to obtain the divergence conditions. High-speed motion pictures at a speed of about 1,400 frames per second were taken of the model during each tunnel test.

TEST PROCEDURE

The tests were conducted in the Langley 9- by 18-inch supersonic flutter tunnel. This tunnel is of the intermittent blowdown-type using fixed nozzle blocks and operating from a high-pressure source to a vacuum. The transonic tests were made by using a slotted test-section nozzle employing a choking device in the diffuser to obtain the desired Mach number in the test section.

The tests were made at approximately constant Mach number and constantly increasing dynamic pressure until the desired results were obtained. The maximum dynamic pressure of the tunnel is limited in the range of these tests to those obtainable with a pressure of 35 pounds per square inch absolute in the test section.

RESULTS AND DISCUSSION

The test results obtained for the basic models are listed in table I(a) and are shown in figure 3 where the dynamic pressure required to produce flutter or divergence is plotted as a function of Mach number. Also shown in figure 3 is a curve showing the sea-level operating conditions of the rocket.

The flutter boundary parallels the operating curve with a small margin of safety at subsonic speeds and then appears to cross over into the operating region at Mach numbers greater than 1.05. The dynamic pressure at the static-divergence boundary appears to be roughly constant within the scatter of the data and crosses into the missile operating region at a Mach number of about 1.1.

The type of flutter encountered was relatively mild and involved predominantly torsional motions as indicated by the flutter frequencies listed in table I(a) and by examination of motions pictures taken during the tests. In some cases when flutter occurred, the dynamic pressure was increased without causing damage to the model until divergence of the overhung leading edge was encountered. After the model diverged, the flutter became less violent or stopped completely. In general, the

divergence produced a permanent deformation which is illustrated by the photograph of a typical model shown in figure 4.

Some possible solutions to the problem have been examined. Results of these tests of modified configurations are listed in table I(b). For one test (test 33) the overhung leading edge was restrained by attaching clips to the tunnel wall. Divergence was eliminated but flutter occurred within the missile operating region. Other models which were about 25 percent and 45 percent thicker than the basic models were tested. No aeroelastic instabilities were encountered within the maximum dynamic pressure to which the tests were extended which, as indicated in figure 3, is well beyond the sea-level operating condition of the ASROC. Tests of configurations with modified plan form and root restraint (see fig. 1(b) and table I(b)) indicate that extending the root clamping plates from the leading edge to the trailing edge eliminated aeroelastic instabilities within the flight boundary. Other configurations with portions of the leading edge unsupported experienced flutter within the flight boundary.

The possible effects of the nondestructive type of flutter of the fins encountered in these tests on the flight path of the ASROC would be difficult to assess. However, it would be expected that the occurrence of divergence would produce large deviations from the intended flight path. In addition to the uncertainties regarding adequacy of model simulation, another question of concern is the possible effects of the relatively large longitudinal accelerations acting on the fins during the boost phase. It would seem that these effects would be small; however, their evaluation is beyond the scope of the present investigation. It may be noted that the U. S. Proving Ground (Dahlgren, Va.) reported in unpublished data that flutter was observed in a tracking film of an ASROC firing; however, the effect on the trajectory was not mentioned.

CONCLUDING REMARKS

The results of the experimental studies (neglecting acceleration effects) on 0.4-scale models of the ASROC rocket-motor fins appear to indicate some aeroelastic instability within the sea-level operating conditions of the missile in the higher Mach number region. The flutter is mild and nondestructive, its effect on the trajectory being difficult to assess. On the other hand, the divergence of the overhung leading edge could produce large trajectory deviations. Results of tests on models about 25 percent and 45 percent thicker than the scaled model and on models with a variation in plan form and with clamping plates extending

the full length of the root chord indicated no aeroelastic instability within the operating conditions of the missile.

Langley Aeronautical Laboratory,
National Advisory Committee for Aeronautics,
Langley Field, Va., July 24, 1958.

TABLE I

EXPERIMENTAL RESULTS

(a) Basic configuration

Test	Model	t, in.	Frequency, cps					M	T, °R	ρ, slugs/cu ft	a, fps	q, lb/sq ft	Legend (a)	Remarks
			f ₁	f ₂	f ₃	f ₄	f _F							
10	BF-4	0.050	114	185	250	340	---	1.30	544	0.00189	988	1,557	D	Diverged mildly Fluttered and then diverged while fluttering Fluttered only; q _{max} reached at 1,290 lb/sq ft Fluttered only Diverged Diverged mildly
16	BF-5	.050	111	178	288	333	150	.81	558	.00345	1,090	1,337	F	
								.81	564	.00484	1,096	1,894	D	
25	BF-8	.050	118	179	---	337	164	1.15	544	.00245	1,023	1,606	F	
								1.15	545	.00297	1,023	1,955	D	
27	BF-9	.050	113	184	296	350	160	.89	549	.00350	1,067	1,576	F	
								.89	549	.00368	1,067	1,655	D	
28	BF-11	.050	117	178	298	340	151	.78	552	.00347	1,088	1,250	F	
								.78	557	.00477	1,095	1,734	D	
29	BF-10	.050	112	169	272	328	149	.61	559	.00410	1,121	823	F	
30	BF-10	.050	115	169	290	320	145	.69	546	.00353	1,097	1,010	F	
31	BF-12	.050	115	187	290	350	---	1.04	548	.00273	1,042	1,598	D	
32	BF-10	.050	113	170	270	320	---	1.30	545	.00206	990	1,707	D	

(b) Modified configurations

Test	Model	t, in.	Frequency, cps					M	T, °R	ρ, slugs/cu ft	a, fps	q, lb/sq ft	Legend (a)	Remarks
			f ₁	f ₂	f ₃	f ₄	f _F							
33	BF-10A	0.050	114	170	---	310	155	1.30	542	0.00183	986	1,507	F	Leading edge restrained at root Root restraint altered by cutting root (see fig. 1(b))
19	BF-7C	.050	113	164	250	300	145	.60	559	.00246	1,123	887	F	
5	BF-2	.072	147	234	400	455	---	1.30	544	.00424	988	3,500	Q	No flutter - no divergence
6	BF-3	.063	137	215	350	410	---	1.30	532	.00378	977	3,060	Q	
18	BF-2	.072	150	233	430	460	---	.60	566	.00552	1,130	1,264	Q	
21	BF-2	.072	148	234	406	460	---	.96	536	.00574	1,044	2,865	Q	
34	BF-3	.063	128	213	352	420	---	1.30	545	.00378	989	3,125	Q	Low damping near maximum conditions No flutter - no divergence (see fig. 1(b) for model modifications)
37	BF-13	.050	150	213	---	392	---	1.30	555	.00356	999	3,000	Q	
38	BF-13A	.050	133	214	---	380	225	1.30	556	.00338	999	2,850	F	Fluttered - no divergence (see fig. 1(b) for model modifications)
39	BF-14	.050	128	184	---	336	162	1.30	552	.00220	995	1,846	F	
40	BF-15	.050	128	197	---	363	172	1.30	548	.00288	992	2,400	F	Fluttered - no divergence

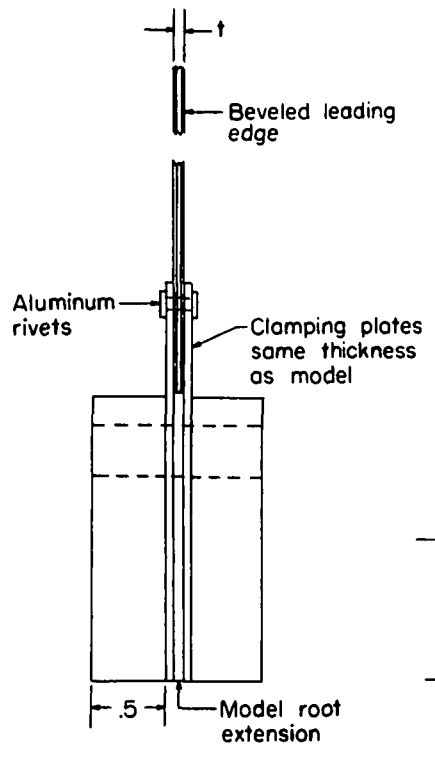
^aThe test-condition legend is as follows:

F - test conditions at flutter

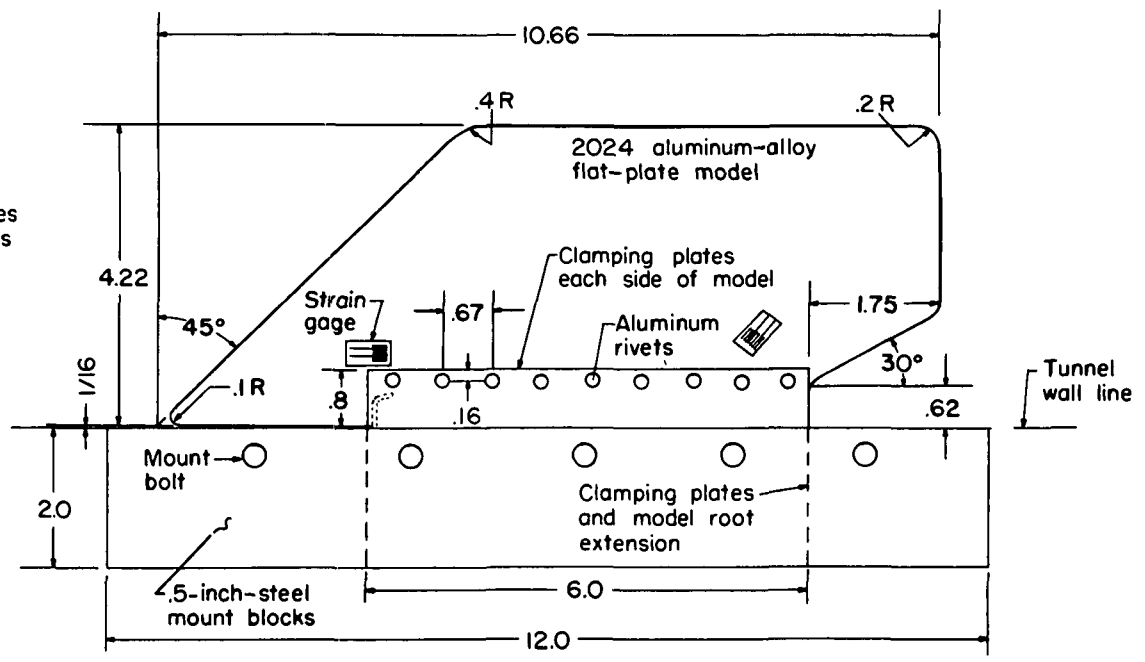
D - test conditions at divergence

Q - maximum test conditions reached without flutter or divergence

Full-scale: all dimensions in inches

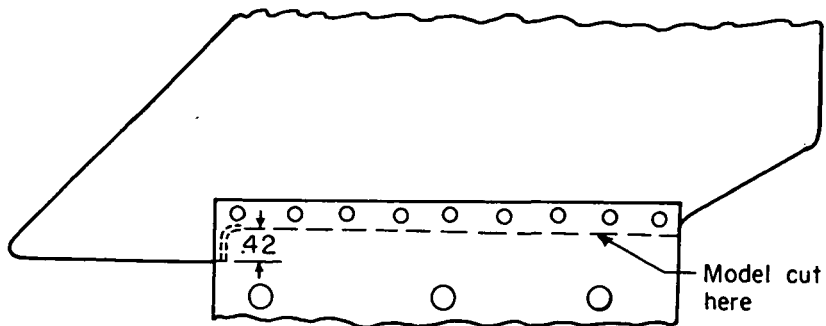


Half-scale: all dimensions in inches

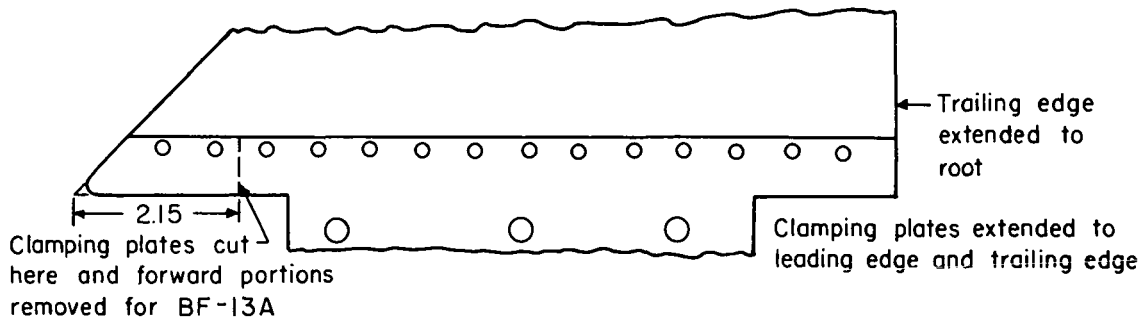


(a) Basic model.

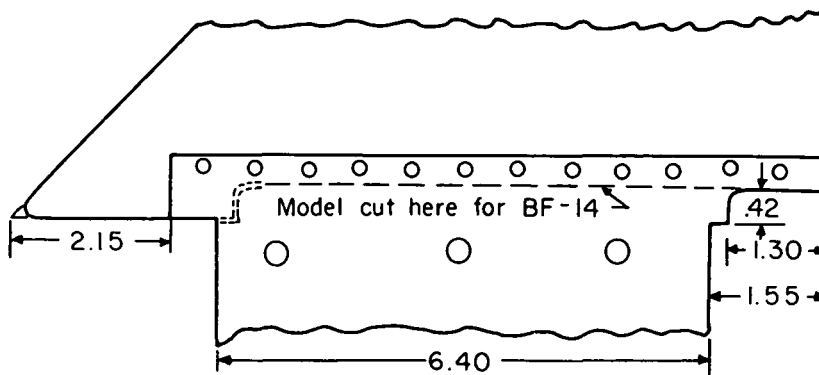
Figure 1.- Model geometry and mounting details.



Model BF - 7C



Models BF - 13 and BF-13A



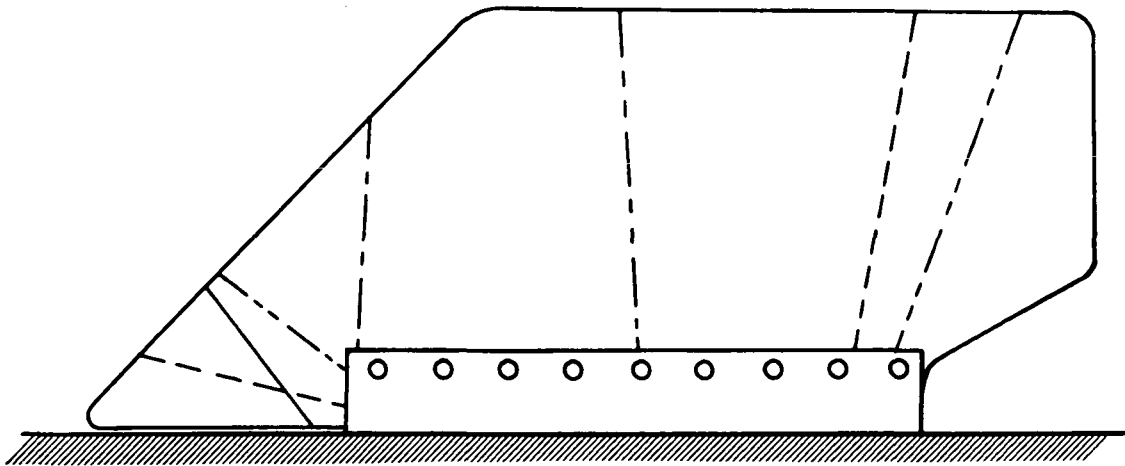
Models BF-14 and BF-15

(b) Modified models. All dimensions are the same as those of the basic model except as noted.

Figure 1.- Concluded.

Mode	Node line
1	—————
2	- - - - -
* 3	- · - · -
4	- · · · -

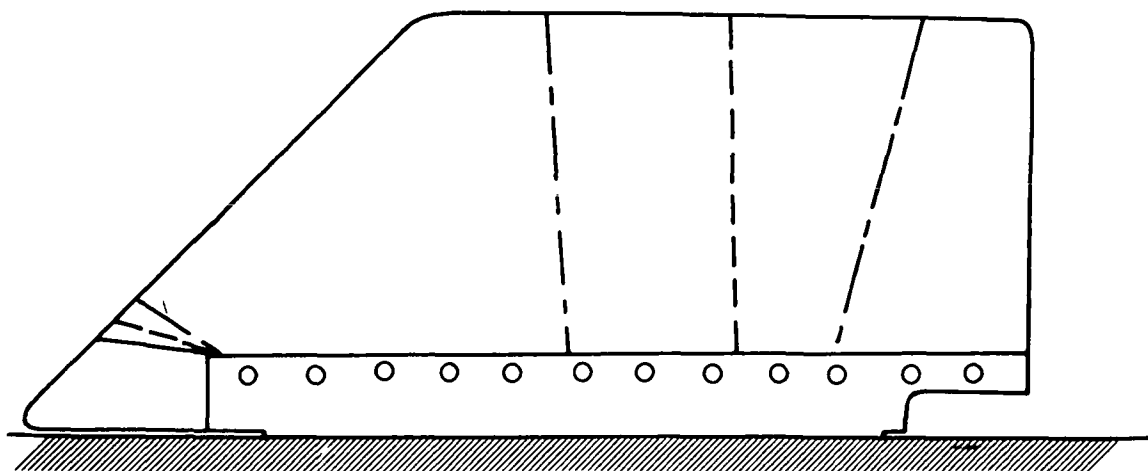
* The third mode appeared to be a leading-edge flapping mode, the rest of the model being motionless.



(a) Basic model.

Figure 2.- Vibration node lines considered typical.

Mode	Node line
1	—————
2	- - - - -
3	——— - -



(b) Modified models. Nodelines for configuration with clamping plates extending length of root chord are same except that there are no node lines near leading edge.

Figure 2.- Concluded.

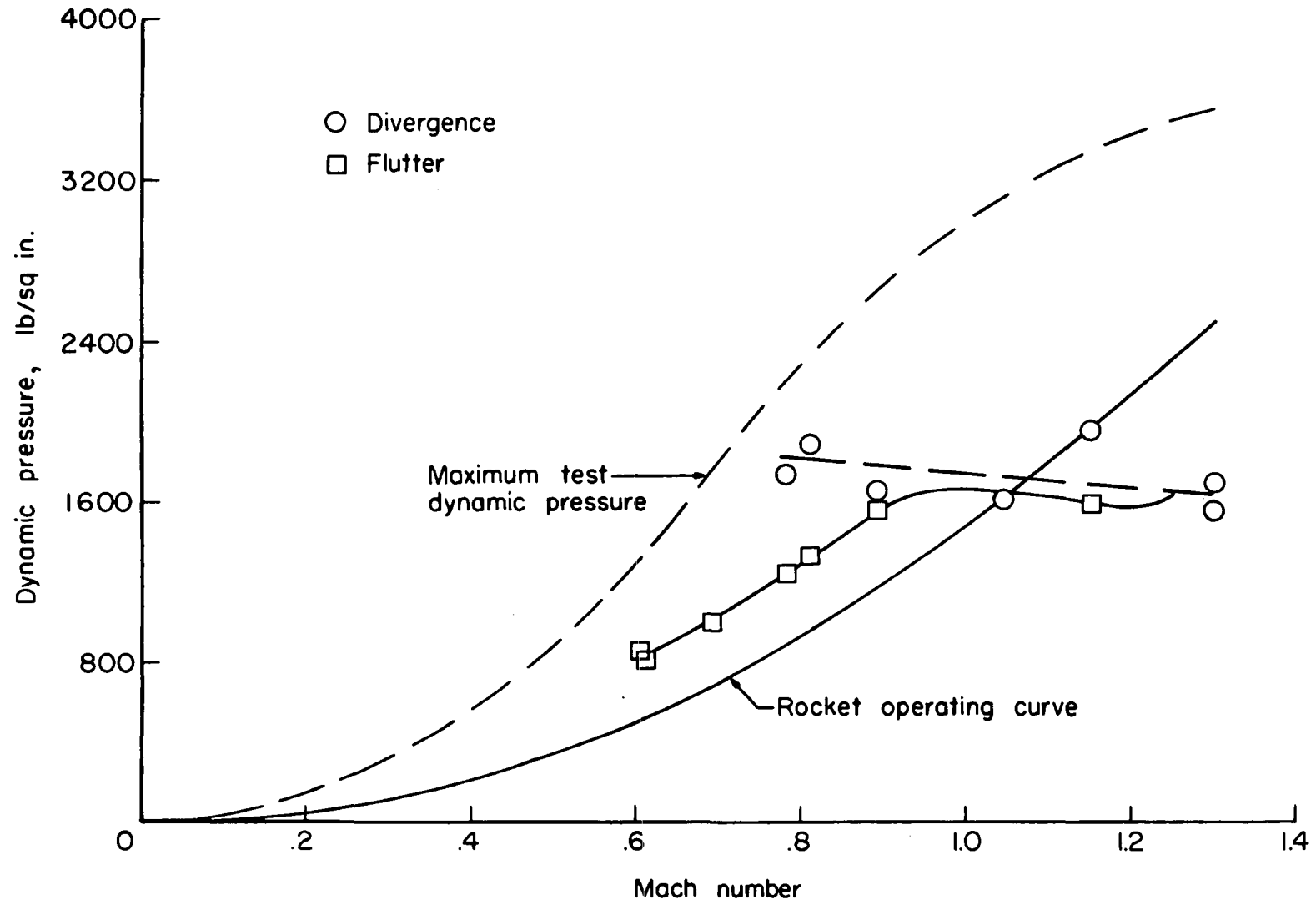


Figure 3.- Flutter and divergence boundaries for rocket-motor fins. Basic models.

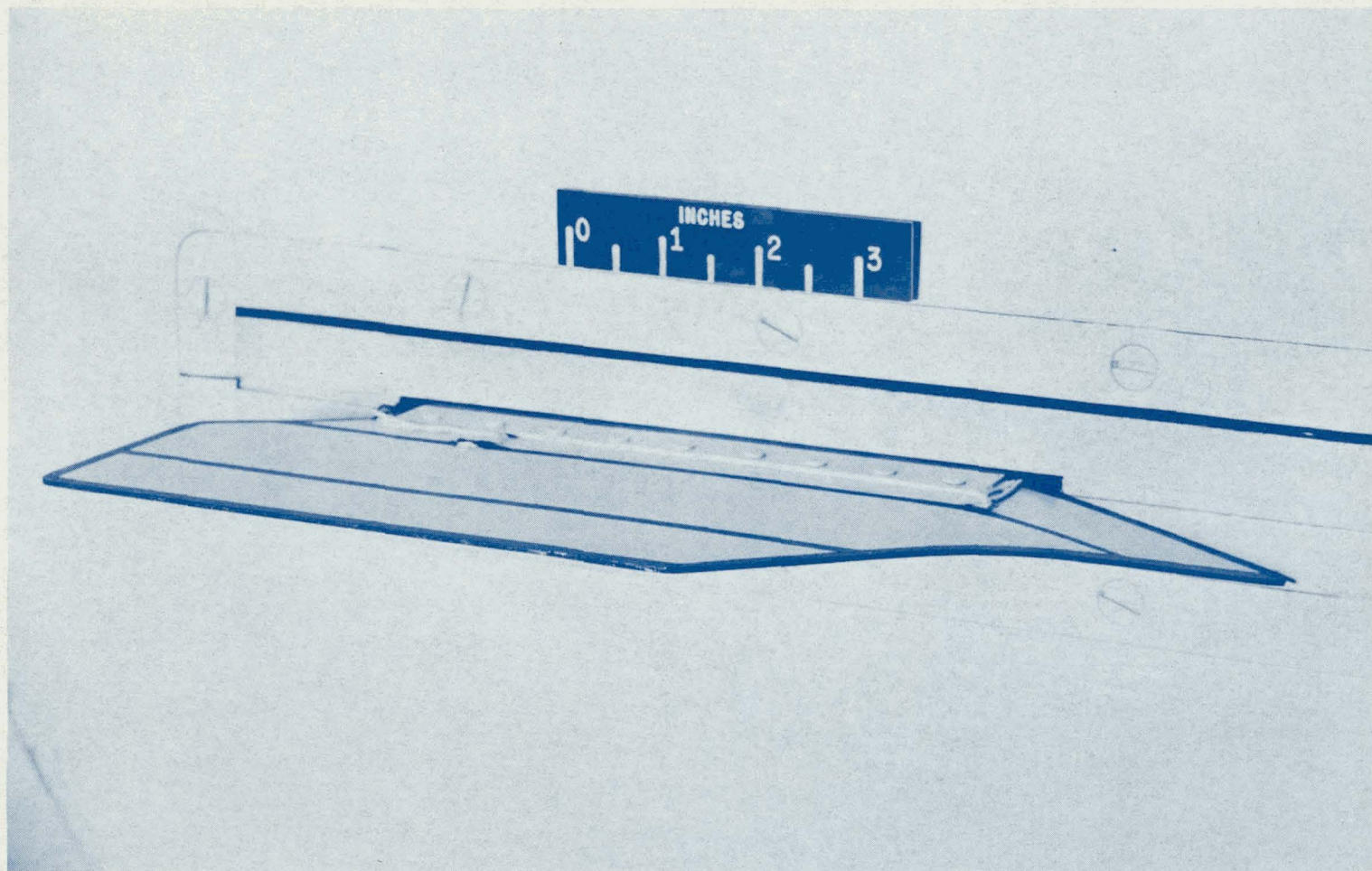


Figure 4.- Photograph of typical diverged model mounted in the Langley 9- by 18-inch supersonic flutter tunnel. L-58-2760



EXPERIMENTAL INVESTIGATION OF FLUTTER AND DIVERGENCE
CHARACTERISTICS OF THE ROCKET-MOTOR FIN
OF THE ASROC MISSILE*

COORD NO. N-AM-66

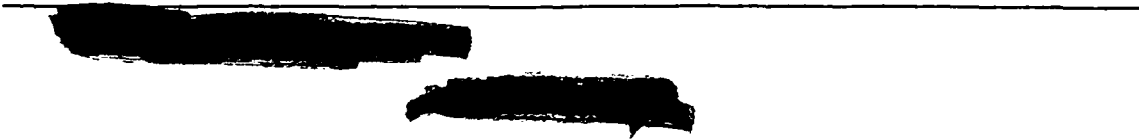
By Gilbert M. Levey and Perry W. Hanson

ABSTRACT

Some 0.4-scale models were investigated in the Langley 9- by 18-inch supersonic flutter tunnel in the Mach number range from about 0.6 to 1.3. Results of this investigation indicate that both divergence of the overhung leading edge and flutter occur within the sea-level operating conditions of the missile at Mach numbers above about 1.0.

INDEX HEADINGS

Mach Number Effects - Wing Sections	1.2.1.8
Missiles, Specific Types	1.7.2.2
Aeroelasticity	1.9
Vibration and Flutter	4.2



EXPERIMENTAL INVESTIGATION OF FLUTTER AND DIVERGENCE

CHARACTERISTICS OF THE ROCKET-MOTOR FIN

OF THE ASROC MISSILE

COORD NO. N-AM-66

Gilbert M. Levey
Gilbert M. Levey

Perry W. Hanson
Perry W. Hanson

Approved: *I. E. Garrick*
I. E. Garrick
Chief of Dynamic Loads Division
Langley Aeronautical Laboratory
mjb(7-24-58)